Fair Charging under Grid Constraints: A Receding-Horizon Game Approach for Electric Vehicle Charging Parks

Benjamin Herrn[1,2], Felix Krabbes[1], Bernd Juris[2] and Rick Voßwinkel[1],

***Abstract*— The large-scale deployment of electric vehicles poses significant challenges for distribution grids, particularly in charging parks with limited network capacity. This paper proposes a fair and grid-aware charging management system based on a receding-horizon game formulation. The coordinated charging problem is modeled as a variational generalized Nash equilibrium (GNE), enabling the allocation of charging power among self-interested vehicles under shared grid constraints. Individual objectives capture price signals, charging smoothness, and terminal energy targets, while electricity network limits are explicitly enforced. In a practice-oriented weekly scenario with limited charging infrastructure, the method enforces the transformer constraint at all times and shows that a 2 h charging-time policy eliminates severe shortfalls above 16 kWh, at the cost of higher shortfalls for some vehicles. These results indicate that the proposed receding-horizon v-GNE formulation provides a transparent mechanism for grid-compliant and fairness-oriented charging coordination.**

I. Introduction

The increasing penetration of electric vehicles (EVs) creates substantial challenges for distribution grids, especially in charging parks connected to feeders or transformers with limited residual capacity. Uncontrolled charging can amplify existing peak loads and cause transformer overloads, voltage deviations, or inefficient grid utilization. Coordinated charging is therefore essential for integrating EV demand while accounting for user behavior, grid constraints, and operational objectives [1], [2], [3].

Charging-park operation is not only a centralized scheduling problem. Each vehicle has user-specific information, such as arrival time, departure time, current battery energy, desired target energy, and preferences regarding cost, smoothness, or battery stress. At the same time, all vehicles are coupled through shared physical constraints, most importantly the available transformer capacity. This gives rise to a multi-agent decision problem in which individual objectives must be coordinated under hard coupling constraints, while limited capacity must be allocated in a transparent and acceptable way [4].

Compared with rule-based charging, centralized MPC, dynamic programming, and distributed optimization, the proposed formulation addresses a different modeling objective. Rule-based methods can enforce aggregate limits, but rely on fixed allocation rules. Centralized MPC and dynamic programming can handle hard constraints, but require a system-level objective and therefore treat the fleet mainly as a cooperative aggregate. Distributed optimization can decompose such cooperative problems, but does not by itself model strategic agents. A generalized Nash equilibrium problem (GNEP), in contrast, keeps individual objectives explicit while coupling agents through shared grid constraints [5], [6], [7].

This paper formulates grid-aware EV charging as a receding-horizon game based on a variational generalized Nash equilibrium (v-GNE). Receding-horizon games combine equilibrium-based multi-agent decision making with repeated feedback-based optimization under updated measurements and forecasts [8], [9]. The variational equilibrium selection is particularly relevant for congested charging parks because active shared constraints induce a common Lagrange multiplier, interpretable as a uniform marginal scarcity price. The contribution is threefold: we formulate charging coordination as a jointly convex finite-horizon GNEP with hard transformer-capacity constraints, embed it into a receding-horizon implementation, and evaluate the framework under active grid constraints, heterogeneous user preferences, limited charging infrastructure, and charging-time restrictions.

II. Receding-Horizon Game

A. Generalized Nash Equilibria and Variational formulation

Consider M agents $\nu \in V := \{1, \dots, M\}$ choosing strategies $u^\nu \in \mathbb{R}^{n_\nu}$ to minimize individual costs $J_\nu(u^\nu, u^{-\nu})$, where $u^{-\nu}$ collects the strategies of all other agents. The stacked vector of all agents' strategies is denoted by $\mathbf{u} \in \mathbb{R}^n$ with $n = n_1 + \cdots n_M$. A vector of strategies $\mathbf{u}^\star$ is called Nash equilibrium, if no agent can further reduce its cost by unilaterally deviating from the equilibrium

$$\forall u^\nu \in U^\nu : \quad J_\nu(u^{\nu,\star}, u^{-\nu,\star}) \leq J_\nu(u^\nu, u^{-\nu,\star}). \tag{1}$$

In a generalized Nash equilibrium, each agent's feasible set $U_\nu(u^{-\nu})$ may depend on the strategies of others. In many resource-sharing systems, feasibility is described by shared coupled constraints, yielding a so-called *jointly convex* structure [5]. Then the feasibility set of all agents can be written as

$$U^\nu = \{u^\nu : (u^\nu, u^{-\nu}) \in \mathbf{U}\} \tag{2}$$

with a compact, convex set $\mathbf{U}$.

Definition 1: The solution of the Variational Inequality (VI) defined by a closed, convex set $\mathbf{U}$ and a function

[1]Benjamin Herrn, Rick Voßwinkel and Felix Krabbes are with the Faculty of Automotive Engineering, University of Applied Sciences Zwickau, Zwickau, Germany {benjamin.herrn.omw, rick.vosswinkel, felix.krabbes.lzc}@whz.de

[2]Bernd Juris is with the Faculty of Computer Science and Automation, Process Optimization Group, Ilmenau University of Technology, Ilmenau, Germany bernd.juris@tu-ilmenau.de

$F : \mathbf{U} \to \mathbb{R}^n$ is a vector $\mathbf{u}$ which solves $F(\mathbf{u})^\top(\mathbf{u} - y) \geq 0$ for all $y \in \mathbf{U}$.

Under convexity and differentiability conditions, a Variational GNE (v-GNE) is the equilibrium associated with a Variational Inequality (VI) over the common feasible set $\mathbf{U}$ as defined in (2) by defining

$$F(\mathbf{u}) = \begin{pmatrix} \nabla_{u^1} J_1(\mathbf{u}) \\ \vdots \\ \nabla_{u^M} J_M(\mathbf{u}) \end{pmatrix}. \tag{3}$$

The set of solutions of the v-GNE is a subset of the solutions of the GNE. For a finite number $m \in \mathbb{N}$ of inequality constraints, collected in $g : \mathbb{R}^n \to \mathbb{R}^m$, the feasibility set is described by

$$\mathbf{U} = \{\mathbf{u} \in \mathbb{R}^n : g(\mathbf{u}) \leq 0\}. \tag{4}$$

Under the assumption of a closed, convex feasibility set and convex cost functions, a v-GNE can be computed through the KKT conditions of the VI formulation. The KKT system takes the form

$$F(\mathbf{u}) + \nabla g(\mathbf{u})^\top \lambda = 0, \tag{5}$$

$$g(\mathbf{u}) \leq 0,\ \lambda \geq 0,\ \lambda^\top g(\mathbf{u}) = 0, \tag{6}$$

where $\lambda \in \mathbb{R}^m$ collects the Lagrange multipliers. This v-GNE solution implies identical Lagrange multipliers for shared, active constraints for all agents, and therefore a uniform marginal "shadow price" for active global constraints [5].

B. Receding-Horizon

We consider discrete time with a sampling period $T_s > 0$ and a finite horizon length $N \in \mathbb{N}$. Let $K := \{0, \ldots, N-1\}$ denote the set of time steps in the prediction horizon.

A RHG is a repeated equilibrium computation over the finite horizon N at each time step. Let x_k denote the measured system state and ϕ_k the exogenous parameters/forecasts (prices, available grid capacity). For each agent, a control sequence

$$(u_k^\nu)_{k\in K} := \{u_0^\nu, u_1^\nu, \ldots, u_{N-1}^\nu\} \tag{7}$$

is computed, such that the joint profile $(\mathbf{u}_k)_{k\in K}$ constitutes an equilibrium of the finite-horizon game, subject to the system dynamics and constraints. Only the first element of the optimal control sequence u_0^ν is implemented. The process repeats in the next time step with updated measurements and forecasts [8], [9].

C. Vehicle Battery Dynamics and Individual Constraints

For each vehicle $\nu \in V$, the state $x_k^\nu \in \mathbb{R}$ denotes battery energy at timestep k. Charging power $u_k^\nu \in \mathbb{R}$ is positive for charging and negative for discharging (if Vehicle to Grid is considered). The energy balance yields

$$x_{k+1}^\nu = x_k^\nu + T_s\, u_k^\nu, \quad \forall k \in K. \tag{8}$$

The model can be extended with efficiencies, but (8) is sufficient for tractable convex formulations.

Algorithm 1: Receding-Horizon Game algorithm

1 **for** $j \leftarrow 0, 1, \ldots$ **do**
2 measure current states $x_0(j)$ and exogenous parameters $\phi_0(j)$ and obtain forecasts $\phi_k(j)$ for $k = 1, \cdots, N-1$
3 Formulate finite-horizon game over $k = 0, 1, \ldots, N-1$ with individual costs J_ν and individual and shared constraints.

$$\forall \nu : \min_{u^\nu}\ J^\nu\big(u^\nu, u^{-\nu}, \phi_k\big)$$

$$\text{s.t.}\quad x_{k+1} = f\big(x_k, u_k^1, \ldots, u_k^M\big)$$

$$u_k^\nu \in U^\nu, \quad k = 0, \ldots, N-1,$$

4 Compute an equilibrium $(\mathbf{u}_k^\star)_{k\in K}$ (v-GNE) of the game.
5 Apply first action: $u_j^\nu \leftarrow u_0^{\nu,\star}(j)$ for all ν.
6 Advance system and shift horizon: $j \leftarrow j + 1$.

For the vehicle-specific constraints, bounds on power and energy

$$u_{\min}^\nu \leq u_k^\nu \leq u_{\max}^\nu, \quad \forall k \in K, \tag{9}$$

$$x_{\min}^\nu \leq x_k^\nu \leq x_{\max}^\nu, \quad \forall k \in K \tag{10}$$

are imposed. Availability windows can be encoded by setting $u_k^\nu = 0$ outside the user-provided interval $[t_{\text{start}}^\nu, t_{\text{end}}^\nu]$ or by tightening bounds in (9).

D. Energy Distribution Grid Constraint

Let $P_{\text{transformer},k}$ denote the power limit for the distribution grid. Let $P_{\text{load},k}$ be the exogenous neighborhood baseload (households/commerce). The residual capacity available for EV charging is

$$P_{\max,k} = P_{\text{transformer},k} - P_{\text{load},k}. \tag{11}$$

Define the aggregate EV power

$$L_k := \sum_{\nu\in V} u_k^\nu. \tag{12}$$

Then the coupling constraints become

$$L_k \leq P_{\max,k}, \quad \forall k \in K, \tag{13}$$

$$L_k \geq P_{\min,k}, \quad \forall k \in K, \tag{14}$$

where $P_{\min,k}$ can represent a lower bound on net injection (e.g., limiting discharging), possibly negative.

Stack the decision variables for the finite horizon as $u^\nu := (u_k^\nu)_{k\in K} \in \mathbb{R}^N$ and $\mathbf{u} := (u^\nu)_{\nu\in V} \in \mathbb{R}^{M\cdot N}$. By eliminating states using (8), energy bounds (10) become affine inequalities in u^ν. Together with (9) and (13)–(14), the joint feasible set is a (nonempty) convex polyhedron.

E. Agent Objectives

Each vehicle ν aims to (i) exploit price signals, (ii) avoid aggressive power profiles (loss/aging proxy), (iii) internalize congestion via an aggregate-load dependent term, and (iv) meet a terminal energy target x^{ν}_{ref}. For the case under consideration here, the only exogenous parameter considered in the cost function is the electricity price $\phi_k = p_k$. A representative convex objective is

$$J_\nu(u^\nu, u^{-\nu}, \phi_k) := \sum_{k\in K} \Big(w_1\, p_k\, T_s\, u^\nu_k + w_2\, (u^\nu_k)^2 + w_3\, L_k\, u^\nu_k \Big) + w_4\, \big(x^\nu_{\text{ref}} - x^\nu_{k+N}\big)^2, \tag{15}$$

with nonnegative weights $w_i \geq 0$. The price signal p_k may be chosen to be mean-free to encode relative incentives without penalizing unavoidable energy purchases. The coupling term $L_k u^\nu_k$ captures that high aggregate load increases marginal stress/cost. The weights may be homogeneous or vehicle-specific (e.g., incentives or priority schemes). The terminal term is a soft service-quality penalty rather than a hard target constraint. It preserves feasibility under scarce capacity, but large values of w_4 may induce more aggressive charging close to the end of the prediction horizon. This trade-off motivates the charging-time policy and occupancy incentives studied in section III-C.

At each sampling instant k, agents solve the coupled optimization game

$$\forall \nu \in V: \quad \min_{u^\nu}\; J_\nu(u^\nu, u^{-\nu}, \phi_k) \quad \text{s.t.} \quad u^\nu \in U^\nu. \tag{16}$$

The constraints, which depend on the strategies of the other agents, defined by (13)–(14), are shared among all agents. The problem is therefore a jointly-convex GNEP and the previously discussed method can be applied. This characterization enables solving equilibria via KKT/VI-based methods rather than nested best responses [5], [6].

The proposed architecture requires a coordination entity, e.g. a charging park operator or local energy management system. At each receding-horizon step, each connected vehicle communicates its current energy state, availability window, charging-power bounds, target energy, and objective weights to the coordinator. The coordinator obtains the exogenous forecasts, i.e. residual grid capacity and price signal, and computes the v-GNE of the finite-horizon game. Only the first charging-power setpoint is communicated back to each vehicle. Vehicles do not need to exchange private information directly with other vehicles. Coupling occurs through the shared grid constraint and the aggregate-load term. Hence, the approach is distributed at the modeling level with agent-specific objectives, but coordinated at the implementation level through a local operator.

F. Numerical Solution

Due to the affine inequality constraints, we can use a smoothed Fischer-Burmeister method [10] to solve for the v-GNE. Complementarity for each scalar pair (a, b) can be encoded by the Fischer–Burmeister function

$$\varphi(a, b) := \sqrt{a^2 + b^2} - a - b, \tag{17}$$

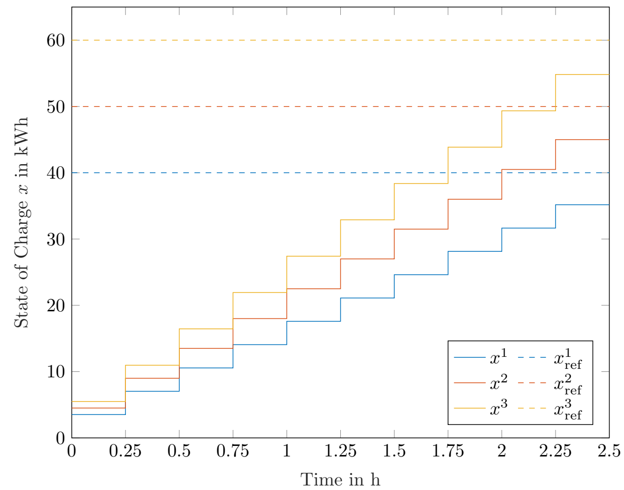

Fig. 1. Vehicle charging state.

where $\varphi(a, b) = 0$ is equivalent to $a \geq 0$, $b \geq 0$, and $ab = 0$. A smoothed variant φ_ϵ yields a semismooth system amenable to Newton-type methods [10]. Applying this elementwise to $(\lambda, -g(\mathbf{u}))$ converts (5)–(6) into a root-finding problem.

III. Case Studies

To quantify charging performance, we report the residual (missing) energy at the end of the respective charging opportunity,

$$\Delta x^\nu := \left| x^\nu_{\text{end}} - x^\nu_{\text{ref}} \right|, \tag{18}$$

where x^ν_{end} denotes the realized battery energy at the end of the considered horizon/availability interval and x^ν_{ref} the target energy at departure. In the following, fairness refers to scarcity fairness. Under symmetric objectives and constraints, scarce charging capacity should lead to equal or near-equal residual energy shortfalls. For heterogeneous weights, unequal shortfalls are interpreted as preference-consistent allocations.

A. Three Vehicles

1) Setup: This scenario isolates the interaction between individual quadratic power penalties, terminal target tracking, and shared grid limits. Three vehicles share identical availability windows, with sampling time $T_s = 0.25\,\text{h}$ and horizon length $N = 10$ (i.e., $2.5\,\text{h}$). Initial energies are idealized as $x^\nu_0 = 0\,\text{kWh}$ for $\nu \in \{1, 2, 3\}$, and target energies are

$$x_{\text{ref}} = (40,\ 50,\ 60)\ \text{kWh}. \tag{19}$$

The objective weights are chosen as $w_1 = 0$, $w_2 = 0.01$, $w_4 = 500$, and heterogeneous coupling weights $\mathbf{w}_3 = (1.2,\ 2.0,\ 2.8)$ to reflect heterogeneous sensitivity to aggregate-load-related penalties. Figure 1 shows the states of the three vehicles over time as well as their energy target.

When the coupling constraint is inactive (sufficient residual grid capacity), the RHG solution approaches the terminal targets but does not fully match them due to the trade-off between target tracking and the penalty on quadratic power and aggregate load. The resulting residual energies are

$$\Delta x = (0.78,\ 0.97,\ 1.16)\,\mathrm{kWh}. \tag{20}$$

When the coupling constraint becomes active, full target satisfaction becomes infeasible. For a constant grid limit of $P_{\max} = 54\,\mathrm{kW}$, the residual energies increase to

$$\Delta x = (4.83,\ 5.00,\ 5.17)\,\mathrm{kWh}, \tag{21}$$

and the heterogeneity in w_3 induces a differentiated allocation: vehicles with larger w_3 accept higher residual energy, consistent with stronger penalization of load-intensive behavior.

2) Fairness Effect under Homogeneous Coupling Weights: To highlight the fairness interpretation of the v-GNE under shared constraints, we repeat the active-constraint experiment with homogeneous coupling weights $w_3^\nu = 2$ for all vehicles. In this case, the residual energies equalize,

$$\Delta x = (5.00,\ 5.00,\ 5.00)\,\mathrm{kWh}, \tag{22}$$

illustrating that, under symmetric preferences for the coupling term, the equilibrium allocates the scarcity in a balanced manner.

B. Practice-Oriented Scenario with a Limited Number of Charging Points

1) Setup and Data Basis: This study evaluates RHG behavior over a realistic weekly profile. The neighborhood baseload $P_{\mathrm{load},t}$ is derived from empirical data from the JenErgieReal-project[1] for a typical summer week (07/15/2024 – 07/21/2024). The transformer rating is set to $P_{\mathrm{transformer}} = 300\,\mathrm{kW}$, and vehicle availability times and durations are aligned with data from the MID study [11]. The considered fleet comprises 42 vehicles with an average weekly energy demand of $64.2\,\mathrm{kWh}$ derived from average annual mileage from [11] and average energy consumption from ADAC Ecotest[2]. The objective weights are fixed to

$$w_1 = 1, \quad w_2 = 0.01, \quad w_4 = 500, \quad w_3 = 2. \tag{23}$$

The prediction horizon is $N = 20$ steps, corresponding to $5\,\mathrm{h}$ with $T_s = 0.25\,\mathrm{h}$. Throughout the case studies, neighborhood baseload and electricity price are treated as perfect forecasts,

$$\hat{P}_{\mathrm{load},k} = P_{\mathrm{load},k}, \qquad \hat{p}_k = p_k, \quad \forall k \in K. \tag{24}$$

This nominal assumption is motivated by the short horizon and the aggregated baseload signal. Since $P_{\max,k}$ is computed from transformer capacity minus uncontrollable load, forecasting available charging capacity reduces to short-term load forecasting. Recent large-scale smart-meter studies report prediction errors below $10\,\%$ for horizons up to $96\,\mathrm{h}$ at feeder, substation, and district levels [12]. Nevertheless, the

[1]real-world laboratory JenErgieReal, grant ID 03EWR016 A-L, https://www.stadtwerke-jena.de/energiewende/jenergiereal.html

[2]ADAC e.V. (Allgemeiner Deutscher Automobil-Club e.V.), https://www.adac.de/rund-ums-fahrzeug/autokatalog/ecotest/

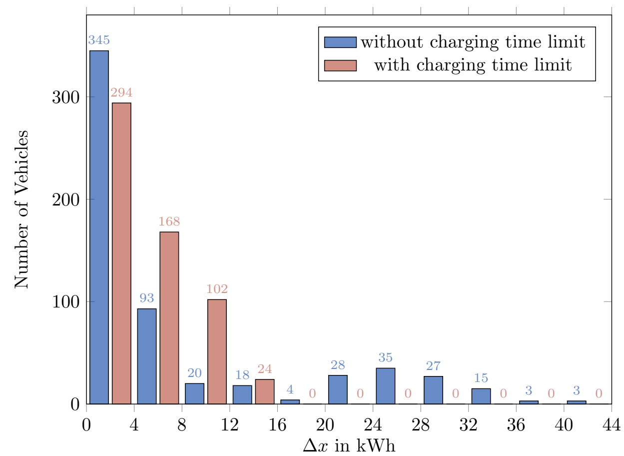

Fig. 2. Histogram of energy shortfall with and without a charging-time limit.

results should be interpreted as nominal closed-loop performance. Robustness against load, price, and arrival/departure uncertainty remains future work.

C. Influence of Limited Charging Duration

1) Limited Charging Infrastructure (Queueing): In the previous scenarios, we assume that all available vehicles can be assigned to a charger. In practice, however, charging facilities provide only a bounded number of charging points. We therefore introduce a limit n_{LS} on the number of vehicles that can be charged simultaneously. If more vehicles become available than there are charging points, a waiting queue forms, and only the subset of plugged-in vehicles participates in the RHG at the respective time step.

Using a 2030-oriented projection with 252 vehicles (corresponding to 20% electrification in the considered setting) and a restricted infrastructure of $n_{\mathrm{LS}} = 20$ charging points, the system exhibits sustained queueing during periods of high availability. Owing to the cost function in (15), each vehicle prefers to exploit its full availability window rather than to increase charging power to meet the energy target earlier. Hence, vehicles have no incentive to charge at higher power as long as their individual availability windows allow meeting the target via slower charging. Although the RHG continues to enforce the grid-coupling constraints, the infrastructure bottleneck becomes the dominant scarcity driver. Consequently, the realized aggregate charging power is no longer limited primarily by $P_{\max,k}$, but by charger occupancy.

2) Additional Charging-Time Limit: To reflect operational policies, we impose a maximum charging duration of $2\,\mathrm{h}$ per charging session. The receding-horizon game algorithm accommodates this naturally if the charging-power bounds in (9) are set to zero for time steps outside the admissible charging-time window. Figure 2 shows the distribution of unmet energy demand (shortfall) Δx^ν relative to the vehicle-specific charging targets. The histogram uses $4\,\mathrm{kWh}$-wide bins, thus, each bar quantifies the number of vehicles whose

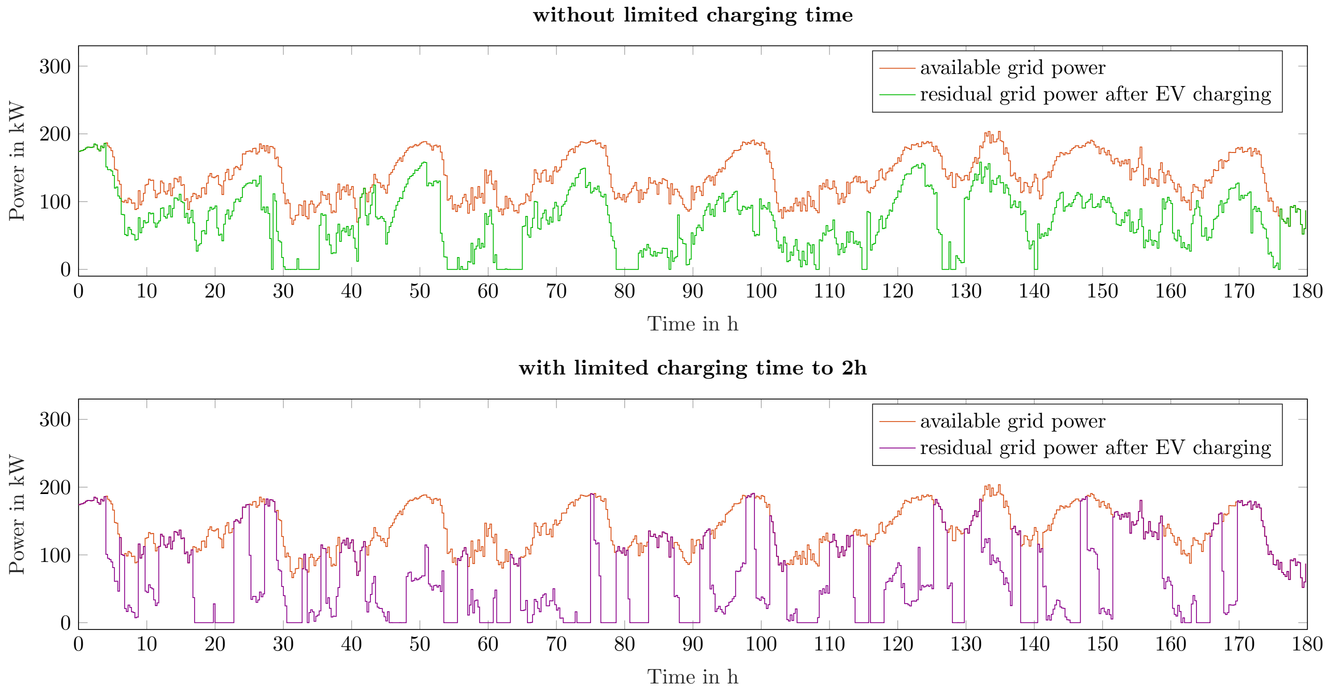

Fig. 3. Comparison of residual grid power with and without charging time limit.

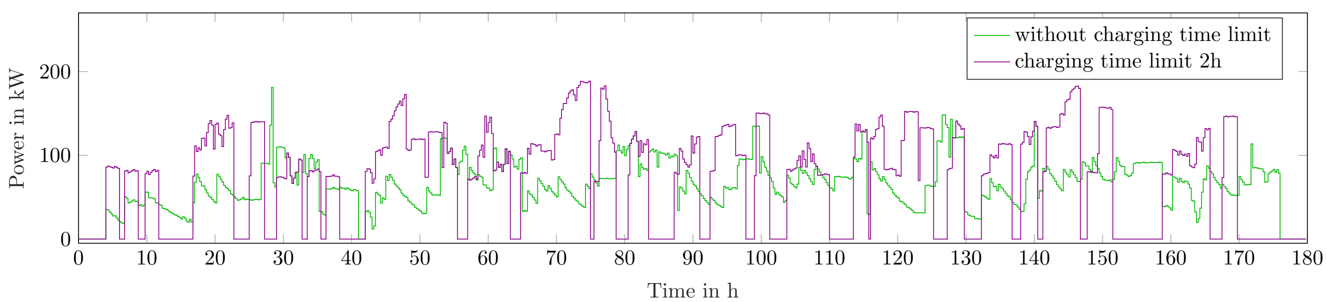

Fig. 4. Aggregate EV power consumption

shortfall falls within the corresponding interval. This representation enables a compact assessment of both the prevalence and the severity of target violations for unconstrained charging and for a charging-time limit of $2\,\mathrm{h}$.

Without a charging-time limit, the concentration of mass in the lowest bins indicates that most vehicles are either fully served or only marginally undercharged, whereas the right tail reveals a subset of vehicles experiencing substantial deficits. This behavior arises because long waiting queues form when vehicles have no incentive to vacate a charging point early, causing some vehicles to wait for most of (or even their entire) availability window. Introducing a charging-time limit substantially reduces queueing and results in no vehicle exhibiting a shortfall exceeding $16\,\mathrm{kWh}$. However, the tighter constraint also leads to slightly larger shortfalls for some vehicles compared to the unconstrained case. Overall, these results indicate that, under a limited number of charging points, either additional time constraints or explicit incentives to charge faster and leave earlier (encoded in the cost function) are required to achieve a fairer and more evenly distributed allocation.

The impact of EV charging on the power grid is shown in Figure 3. The available grid power $P_{\max,k}$, as defined in (11), is presented alongside the residual grid power after EV charging,

$$P_{\text{residual},k} = P_{\max,k} - L_k.$$

A residual power of zero indicates that the maximum available grid capacity is fully utilized for charging. Conversely, equality of available power $P_{\max,k}$ and residual grid power $P_{\text{residual},k}$ indicates that no vehicle is charging at time step k. Figure 4 depicts the aggregate charging power L_k for both cases. With a charging-time limit, vehicles draw higher peak charging power to satisfy their energy requirements within a shorter time window compared to the unconstrained scenario.

a) Computational effort and real-time feasibility.: The largest simulated instance considered in this study comprises 252 vehicles and $n_{\mathrm{LS}} = 20$ charging points. Although the implementation was not optimized and combines Python with MATLAB/Simulink components, the computation time remained below one minute per receding-horizon update in all simulation steps. Since the sampling time is $T_s = 0.25\,\mathrm{h}$, this leaves a substantial margin relative to the available 15-minute control interval. Moreover, the number of simultaneously optimized agents is naturally bounded in the considered application, because the coordination problem is local to one charging park and only vehicles assigned to a charging point participate in the game. These observations indicate that the proposed RHG-vGNE scheme is compatible with real-time operation for charging-park-scale instances, although optimized implementations and systematic runtime benchmarks remain future work.

IV. Conclusion

This paper presented a receding-horizon v-GNE framework for fair and grid-aware EV charging under hard shared network constraints. In the three-vehicle scenario, active grid constraints lead to nearly balanced residual energies, and under homogeneous coupling weights the residual shortfall is exactly equalized at $5.00\,\mathrm{kWh}$ per vehicle. This supports the interpretation of the common multiplier in the variational equilibrium as a uniform scarcity signal.

In the larger charging-park scenario, grid feasibility alone is not sufficient when the number of physical charging points is limited. Without occupancy incentives, vehicles may remain connected for long periods, causing queue-induced shortfalls for other users. A 2-h charging-time policy mitigates this effect and eliminates severe shortfalls above $16\,\mathrm{kWh}$, but can also increase shortfalls for some users.

The main limitations are the deterministic forecast assumption, the simplified linear battery-energy model, and the absence of a numerical performance benchmark against centralized MPC, dynamic programming, rule-based scheduling, or cooperative distributed optimization. Future work can address robust and stochastic forecast models, explicit occupancy pricing, optimized solver implementations, and systematic runtime benchmarks in operational charging parks.

Acknowledgment

Funding for this contribution was provided through the 'autonomous2grid' project under grant ID 100649620 financed by the European Union, and tax funds from the Saxon/Germany parliament's approved budget.

References

[1] R. Zaino, V. Ahmed, A. M. Alhammadi, and M. Alghoush, "Electric vehicle adoption: A comprehensive systematic review of technological, environmental, organizational and policy impacts," *World Electric Vehicle Journal*, vol. 15, no. 8, p. 375, 2024. DOI: 10.3390/wevj15080375.

[2] M. Shariatzadeh, M. A. R. Lopes, and C. H. Antunes, "Electric vehicle users' charging behavior: A review of influential factors, methods and modeling approaches," *Applied Energy*, vol. 396, p. 126 167, 2025. DOI: 10.1016/j.apenergy.2025.126167.

[3] S. G. Motlagh, J. Oladigbolu, and L. Li, "A review on electric vehicle charging station operation considering market dynamics and grid interaction," *Applied Energy*, vol. 392, p. 126 058, 2025. DOI: 10.1016/j.apenergy.2025.126058.

[4] C.-Y. Chung, J. Chynoweth, C. Qiu, C.-C. Chu, and R. Gadh, "Design of fair charging algorithm for smart electrical vehicle charging infrastructure," in *Proceedings of the 2013 International Conference on ICT Convergence (ICTC)*, IEEE, 2013, pp. 527–532. DOI: 10.1109/ICTC.2013.6675413.

[5] F. Facchinei and C. Kanzow, "Generalized Nash Equilibrium Problems," *Annals of Operations Research*, vol. 175, pp. 177–211, 2010. DOI: 10.1007/s10479-009-0653-x.

[6] F. Facchinei, A. Fischer, and V. Piccialli, "On generalized nash games and variational inequalities," *Operations Research Letters*, vol. 35, no. 2, pp. 159–164, 2007. DOI: https://doi.org/10.1016/j.orl.2006.03.004.

[7] C. Cao and B. Chen, "Generalized nash equilibrium problem based electric vehicle charging management in distribution networks," *International Journal of Energy Research*, vol. 42, no. 15, pp. 4584–4596, 2018. DOI: 10.1002/er.4194.

[8] S. Hall, G. Belgioioso, D. Liao-McPherson, and F. Dörfler, "Receding Horizon Games with Coupling Constraints for Demand-Side Management," in *2022 IEEE 61st Conference on Decision and Control (CDC)*, Dec. 2022, pp. 3795–3800. DOI: 10.1109/CDC51059.2022.9992497.

[9] S. Hall, G. Belgioioso, F. Dörfler, and D. Liao-McPherson, "Stability certificates for receding horizon games," *IEEE Transactions on Automatic Control*, vol. PP, pp. 1–8, Jan. 2025. DOI: 10.1109/TAC.2025.3647314.

[10] D. Liao-McPherson, M. Huang, and I. Kolmanovsky, "A Regularized and Smoothed Fischer–Burmeister Method for Quadratic Programming With Applications to Model Predictive Control," *IEEE Transactions on Automatic Control*, vol. 64, no. 7, pp. 2937–2944, Jul. 2019. DOI: 10.1109/TAC.2018.2872201.

[11] J. Belz et al., "Mobilität in deutschland – mid 2023 — ergebnisbericht," infas Institut für angewandte Sozialwissenschaft GmbH, 2025.

[12] H. Li, M. Heleno, W. Zhang, K. Sun, L. Rodriguez Garcia, and T. Hong, "A cross-dimensional analysis of data-driven short-term load forecasting methods with large-scale smart meter data," *Energy and Buildings*, vol. 344, p. 115 909, 2025, ISSN: 0378-7788. DOI: https://doi.org/10.1016/j.enbuild.2025.115909.